The Journal of Immunology

Nuclear Autoantigen Translocation and Autoantibody Opsonization Lead to Increased Dendritic Cell Phagocytosis and Presentation of Nuclear Antigens: A Novel Pathogenic Pathway for Autoimmunity?

Lorenza Frisoni, Lenese Mcphie, Lucrezia Colonna, Uma Sriram, Marc Monestier, Stefania Gallucci and Roberto Caricchio

J Immunol 2005; 175:2692-2701; ;
doi: 10.4049/jimmunol.175.4.2692
http://www.jimmunol.org/content/175/4/2692

The Journal of Immunology is published twice each month by
The American Association of Immunologists, Inc.,
1451 Rockville Pike, Suite 650, Rockville, MD 20852

Print ISSN: 0022-1767 Online ISSN: 1550-6606.

Nuclear Autoantigen Translocation and Autoantibody Opsonization Lead to Increased Dendritic Cell Phagocytosis and Presentation of Nuclear Antigens: A Novel Pathogenic Pathway for Autoimmunity?[1]

Lorenza Frisoni,* Lenese Mcphie,* Lucrezia Colonna,† Uma Sriram,† Marc Monestier,‡ Stefania Gallucci,[2†] and Roberto Caricchio[2,3*]

Autoreactivity in lupus requires the delivery of autoantigens to APCs in a proinflammatory context. It has been proposed that apoptotic cells are a source of lupus autoantigens and targets for autoantibodies. Using a histone H2B-GFP fusion protein as traceable Ag, we show here that lupus autoantibodies, directed against nuclear autoantigens, can opsonize apoptotic cells, enhance their uptake through induction of proinflammatory FcγR-mediated phagocytosis, and augment Ag-specific T cell proliferation by increasing Ag loading. Apoptotic blebs and bodies seemed to be a preferred target of DC phagocytosis, via both "eat-me signals" and FcγR-mediated mechanisms; furthermore, inhibition of nuclear Ag redistribution, by blockade of chromatin fragmentation, could stop binding and opsonization of apoptotic cells by autoantibodies, and inhibited Fcγ-R-mediated enhancement of phagocytosis. Our results suggest that DC uptake of opsonized histones and other nuclear Ags from apoptotic cells is a novel pathway for the presentation of nuclear Ags in a highly inflammatory context. Blockade of chromatin fragmentation in lupus is a potential therapeutic approach, which could theoretically limit DC access to autoantigens delivered in proinflammatory context, while leaving available for tolerization those delivered in a noninflammatory context. *The Journal of Immunology,* **2005, 175: 2692–2701.**

Systemic lupus erythematosus (SLE)[4] is an autoimmune disease characterized by the production of autoantibodies against self-Ags (1). In this study, we address the pathways by which lupus-specific self-Ags (SLE-autoantigens) are delivered to the immune system.

Apoptotic cells have been proposed as a possible source of nuclear SLE-autoantigens (2). Infusion of large numbers of apoptotic cells in normal mice (3), or defects in the clearance machinery of apoptotic cells, such as those in mice knocked out for mer (4), C1q (5), complement receptor 2 (6), serum amyloid protein (7), DNase I (8), transglutaminase 2 (9), CD31 (10), or milk fat globule epidermal growth factor 8 (11), lead to lupus-like manifestations, especially nuclear autoantibody production and glomerulonephritis (for review, see Ref. 12). These results suggest that apoptotic cells, if not promptly cleared, could become a source of lupus nuclear autoantigens.

During apoptosis, cells go through dramatic morphological changes (13). The cells round up and form blebs (14). The formation of blebs and apoptotic bodies has been regarded as a mechanism of easing the disposal of apoptotic cells by neighboring cells and scavengers, such as scavenger macrophages (15). We hypothesized that apoptotic blebs and bodies are the right size for a delivery system of Ags to APCs, such as dendritic cells (DCs). Our hypothesis is supported by the fact that DCs acquire Ags from apoptotic cells (16, 17) and yet are often much smaller than the surrounding cells, such as in skin; therefore, the uptake of an entire dying cell would be very unlikely. In addition, the nuclear membrane, chromatin fragments, and other nuclear Ags are translocated, concentrated, and exposed in blebs on the cell surface membrane of apoptotic cells (18–21). We report here the first evidence for a direct immunological consequence of nuclear lupus autoantigen redistribution into apoptotic blebs and bodies: the opsonization by autoantibodies that leads to FcγR-mediated phagocytosis and enhanced Ag presentation.

Under physiologic conditions, phagocytosis of apoptotic cells is mediated by "eat-me signals," which are exposed during the early phases of apoptosis (22) and recognized by phagocytic receptors, such as CD36 and $\alpha_v\beta_5$ (23). Ultimately, APCs present self-Ags from apoptotic material in either a tolerogenic or immunogenic way, depending on the activation state of APCs and the surrounding inflammatory environment (16, 17).

In the present paper, we used a histone 2B (H2B)-GFP fusion protein as a traceable autoantigen and found that apoptotic cells, by exposing nuclear autoantigens on the cell surface, allowed autoantibodies, specific of lupus, to opsonize apoptotic cells, especially

*Division of Rheumatology, Department of Medicine, University of Pennsylvania, and †Laboratory of Dendritic Cell Biology, Division of Rheumatology, Department of Pediatrics, The Children's Hospital of Philadelphia, Philadelphia, PA 19104; and ‡Department of Microbiology and Immunology, Temple University School of Medicine, Philadelphia, PA 19140

Received for publication February 2, 2005. Accepted for publication May 30, 2005.

The costs of publication of this article were defrayed in part by the payment of page charges. This article must therefore be hereby marked *advertisement* in accordance with 18 U.S.C. Section 1734 solely to indicate this fact.

[1] This work was supported in part by the Arthritis Foundation (Young Investigator Award to R.C.); American Heart Association (Scientific Development Grant to R.C.); Lupus Foundation, Southeastern Pennsylvania (to S.G.); and the National Institutes of Health (NIH) (NIH/National Institute of Arthritis and Musculoskeletal and Skin Diseases Grant AR048126 to R.C. and NIH/National Institute of Allergy and Infectious Diseases Grant AI049892 to S.G.).

[2] S.G. and R.C. contributed equally to this paper.

[3] Address correspondence and reprint requests to Dr. Roberto Caricchio, Division of Rheumatology, University of Pennsylvania, 751 BRB II/III, 421 Curie Boulevard, Philadelphia, PA 19104. E-mail address: rocarri2@mail.med.upenn.edu

[4] Abbreviations used in this paper: SLE, systemic lupus erythematosus; DC, dendritic cell; H2B, histone 2B; KO, knockout; ROCK I, Rho-associated kinase I; rEGFP, recombinant enhanced GFP; AxV, annexin V; PI, propidium iodide; Ph.I., phagocytic index; MFI, mean fluorescence intensity.

0022-1767/05/$02.00

their fragments as bodies or blebs, promote their phagocytosis, and increase autoantigen presentation by APCs. The inhibition of nuclear Ag redistribution could stop binding and opsonization of apoptotic cells by autoantibodies and, therefore, inhibit FcγR-mediated enhancement of phagocytosis.

In this work, we propose a novel pathogenic role for autoantibodies in maintaining and amplifying the autoimmune response. These insights may provide new potential therapeutic targets in SLE.

Materials and Methods

Mice

C57BL/6 RAG-knockout (KO) (RAG-N12) mice were purchased from The Jackson Laboratory. Mice were bred and maintained in accordance with the guidelines of the University Laboratory Animal Resource Office of the University of Pennsylvania and the Children's Hospital of Philadelphia. C57BL/6 mice were immunized with 10 μg of purified recombinant enhanced GFP (rEGFP) protein (BD Clontech) and CFA. Before injection, rEGFP protein was diluted in a total volume of 50 μl of PBS and emulsified with an equal volume of CFA for 30 min at 4°C.

Dendritic cells

C57BL/6 RAG-KO were used as source of bone marrow-derived DCs as previously described (17). DCs derived from bone marrow of C57BL/6 RAG-KO behave identically to those from normal mice (17).

Bone marrow precursors were seeded in 24-well dishes at a concentration of 1×10^6 cells/ml in 10% FBS complete IMDM containing 3 ng/ml GM-CSF and 2.5 ng/ml IL-4 (BD Pharmingen) and used at days 6–9 of culture (17).

Keratinocyte transfection and induction of apoptosis

The human epidermoid carcinoma cell line A431 (American Type Culture Collection) was stably transfected with the pBOS-H2BGFP vector (BD Pharmingen) carrying the sequence for the human histone H2B tagged with GFP fusion protein (K/H2B-GFP). Cells were transfected with Superfect (Qiagen), according to the manufacturer's instructions. Transfection stability was obtained with blastacidins at a concentration of 5 μg/ml for the first week and then maintained to 2.5 μg/ml.

K/H2B-GFP cells were cultured in complete DMEM medium (10% FBS, glutamine, sodium pyruvate, MEM nonessential amino acids, antibiotics). To induce apoptosis, cells were plated at 2×10^5/ml in six-well plates the previous day and irradiated with 15 mJ/cm^2 using two FS-20 sun lamps (emitting most of their energy in the UVB range (290–320 nm), with an emission peak of 310 nm). The dose was determined with an IL-1700 research radiometer (International Light). In some experiments, a dose of 80 mJ/cm^2 was used to induce necrosis (24). To inhibit DNA fragmentation during apoptosis, K/H2B-GFP cells were incubated with 50 μM Rho-associated kinase I (ROCK I) inhibitor Y27632 (Calbiochem), starting at least 30 min before UVB treatment. Cells were washed twice with PBS before being added to DCs, to eliminate any residual Y27632.

Apoptotic blebs and bodies of different size were separated by serial centrifugation, as previously described (25) with the following modifications: apoptotic cells were collected 5 h after UVB irradiation and were centrifuged at $60 \times g$. At this low centrifugation speed, intact cells, cells in the apoptotic "round phase" (14), and very large bodies could be pelleted. The supernatant was then further centrifuged at $250 \times g$ to isolate small bodies and blebs. To standardize the amount of apoptotic material, total protein content of both pellets was measured with BCA Protein Assay (Pierce Biotechnology) according to the manufacturer's instructions. Both pellets, diluted to attain equal protein concentrations, were incubated with DCs to evaluate the relationship between the size of small apoptotic bodies and blebs, and DC phagocytic capacity. The amount of H2B-GFP fusion protein contained in the small apoptotic bodies and blebs and in the apoptotic cells was also evaluated by flow cytometry.

Test of phagocytosis

DCs were used between days 6 and 9 of culture, a period during which emerging DCs are highly phagocytic (17). Apoptotic K/H2B-GFP were collected and incubated with DCs in 2 ml of total medium for 2 h at 37°C. We performed a dose-response curve in which the number of DCs and the amount of apoptotic cells varied. Initial experiments demonstrated that a 2:1 and a 1:1 ratio of DCs/apoptotic cells resulted in an optimal phagocytic capability. We have therefore used these ratios. Opsonization was achieved by preincubating apoptotic K/H2B-GFP with a mouse monoclonal IgG2a Ab (LG2.2; derived from the autoimmune MRL/*lpr* mouse and directed against histone H2B (26)) for 30 min at room temperature in PBS plus 3% BSA at 100 μg/ml. As an isotype control, an irrelevant mouse monoclonal IgG2a was used at the same concentration. Opsonized cells were then washed in PBS and incubated with DCs.

A rat anti-mouse CD16/CD32 (10 μg/ml; anti-FcγII/IIIR; clone 2.4G2; BD Pharmingen) was used to block the FcγR on DCs. Treatment of DCs with 2.4G2 Ab was initiated 30 min before adding apoptotic cells.

Flow cytometry. Phagocytosis was measured by the percentage of CD11c-positive cells that were also GFP positive (27). The phagocytic index (Ph.I.), as an amount of phagocytosed bodies per cell, was determined as follows: mean fluorescent intensity (MFI) of the CD11c$^+$GFP$^+$ cells (MFI-GFP) multiplied by the percentage of CD11c$^+$GFP$^+$ (CD11c-GFP) cells: Ph.I. = ((MFI-GFP $\times$ CD11c-GFP)/100).

Confocal microscopy. Phagocytosis was evaluated by randomly counting 100 DCs per well at $\times$1200 with oil immersion. Percentage of phagocytosis was calculated counting DCs that contained at least one ingested apoptotic body. The Ph.I. was expressed as percentage of phagocytosis (CD11c-GFP) multiplied by the mean number of phagocytosed bodies per DC (ΔDC): Ph.I. = ((CD11c-GFP $\times$ ΔDC)/100). Apoptotic bodies that were attached and not internalized were also independently counted and constituted <5% in all conditions tested.

FACS staining

DCs and apoptotic cells were collected in cold PBS, washed, incubated for 10 min with 2.4G2, and then stained for 30 min with the following mAbs (BD Pharmingen): biotin- or allophycocyanin-conjugated hamster anti-mouse CD11c, PE- rat anti-mouse B7.2 and B7.1, FITC hamster anti-mouse CD40, and anti-FcγR Abs. After two washes, an additional 20-min incubation with streptavidin-allophycocyanin or streptavidin-Alexa (647) was performed to detect biotinylated Abs. After staining, cells were washed in PBS, fixed in 1% formaldehyde in PBS, and analyzed on a BD Biosciences FACSCalibur, or by confocal microscopy.

Annexin V (AxV) binding, propidium iodide (PI) permeability, and cell cycle analysis were performed as previously described (24). Apoptotic cells were also stained with the monoclonal LG2.2 anti-histone H2B Ab described above and biotinylated rabbit anti-mouse Ig. Streptavidin-PE or streptavidin-Alexa (647) were used to analyze the binding by flow cytometry and confocal microscopy, respectively.

Nuclei preparation, total histone extraction, and anti-GFP Western blot

To extract histones, K/H2B-GFP cells were washed with PBS, resuspended in working mannitol buffer (10^7–10^8 cells/ml), and then incubated on ice for 10 min. After incubation, nuclei were isolated using a tight-fitting pestle. The samples were then spun at $5000 \times g$ for 12 min. The pellet, which contained the nuclei, was washed twice in mannitol buffer and resuspended in micrococcal nuclease complete digestion buffer. Micrococcal nuclease (USB) was added, and chromatin was digested at 37°C for 5 min. EDTA was added to 5 mM to end digestion.

Chromatin was then purified by a sucrose gradient, as previously described (28). Fractions of 1 ml were collected and analyzed for nucleosomal DNA (gel electrophoresis, not shown) and histone content (see below).

Chromatin preparations were then resuspended in a 2.2 M sulfuric acid solution and incubated for 20 min. After incubation, the sample was mixed and allowed to settle, and the supernatant containing the histones was collected. After the addition of 100% TCA at a ratio of 1:4, the mixture was then incubated on ice for 30 min to precipitate the histones. Samples were spun at $10{,}000 \times g$ for 20 min at 4°C. Ethanol (100%) plus 1% sulfuric acid was added to the precipitated histones, which were then spun at $10{,}000 \times g$ for 10 min. Samples were washed twice in ethanol, spun at $10{,}000 \times g$ for 5 min, and then air-dried. The histone pellet was dissolved in Laemmli buffer.

Histones were separated on a 15% SDS-PAGE gel and were then visualized by Coomassie blue staining or transferred onto nitrocellulose membrane. Blots were probed with mouse monoclonal anti-GFP (Santa Cruz Biotechnology) and detected with anti-mouse Ig, HRP conjugated.

Anti-GFP ELISA

The titer of anti-GFP Ab was assayed in sera collected from C57BL/6 mice immunized 2 wk earlier. Ninety-six-well ELISA microplates were coated with rEGFP (1 μg/ml in 1$\times$ BBS) overnight at 4°C and blocked for 1 h with blocking solution (1$\times$ BBS containing 3% BSA and 1% Tween 80). Sera were diluted 1/250 in BBT (1$\times$ BBS containing 0.5% BSA and 0.4%

Tween 80) and incubated for 2 h at 4°C. As a standard curve, serial dilutions of anti-GFP Ab (Sigma-Aldrich) were used. The plate was then incubated with a secondary Ab (goat anti-mouse IgG-biotin, generated in our laboratory) at 0.25 μg/ml in BBT, followed by incubation with avidin alkaline phosphatase (Sigma-Aldrich). Both incubations were conducted at 4°C for 2 h. The plate was washed five times with 1× BBS between incubations.

Phosphatase substrate (Sigma-Aldrich) was added at 1 mg/ml in 0.01 M diethanolamine (pH 9.8) and incubated at room temperature. The plate was read with an Emax Precision Microplate Reader (Molecular Devices).

T cell proliferation

CD4-positive cells were isolated by negative selection from spleen and lymph nodes of C57BL/6 mice previously immunized with GFP in CFA (see above). Spleen and lymph node cells were depleted of $CD8^+$, MHC II^+, and $B220^+$ cells by magnetic sorting with microbeads (Miltenyi Biotec) following manufacturer recommendations. $CD4^+$ cells were then washed twice and resuspended in PBS at $<10^7$ cells/ml, added with the same volume of CFSE solution in PBS (1 μl/ml of a 5 mM CFSE stock solution), and rocked for 5 min. A 10% FBS DMEM medium was added to stop the labeling reaction. Cells were washed and seeded in 96-well round-bottom plates at a concentration of 1.5×10^5 cells/well together with 1.5×10^4 DCs (29). Twenty-four hours before this culture, these DCs had phagocytosed apoptotic cells, as described in the phagocytosis test section, and then had been transferred to induce maturation (17). $CD4^+$ cells were then harvested at 72 h and stained with anti-CD4 Ab, allophycocyanin-conjugated.

Confocal microscopy

Live imaging. K/H2B-GFP cells were cultured in glass-bottom culture dishes (MatTek). Cells were then UVB irradiated and imaged with a Nikon TE300 scanning confocal microscope, equipped with Nomarski differential interphase contrast optics, coupled to the Bio-Rad Radiance 2000 laser. Cells were maintained at constant temperature (37°C) in an open perfusion microincubator regulated by a temperature controller (Harvard Apparatus). Stacks of images with a thickness of 0.5 mm were collected with a ×60 oil objective and a ×2.5 digital zoom, and analyzed with Laser Sharp 2000 software (Bio-Rad).

For the phagocytosis experiments, DCs were seeded onto apoptotic K/H2B-GFP cells cultured in glass-bottom dishes (MatTek). Cells were maintained at constant temperature as above. Single images were then collected every 30 s for up to 2 h with a ×60 oil objective and ×2.5 digital

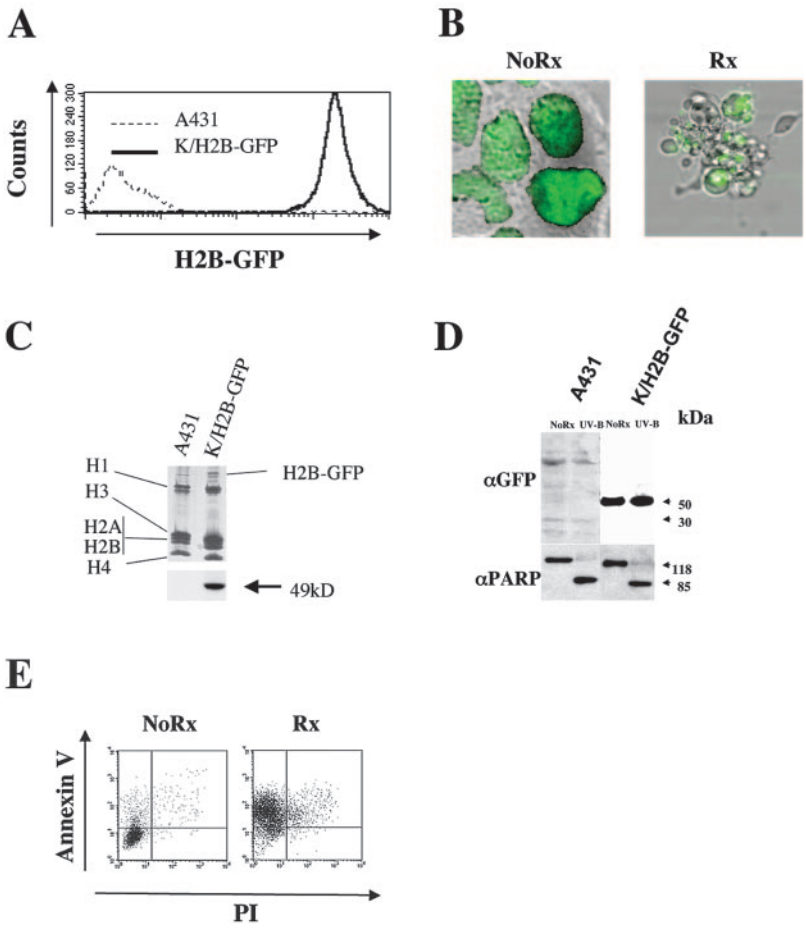

FIGURE 1. UVB induced apoptosis in K/H2B-GFP cells: membrane flipping, DNA fragmentation, and Ag redistribution. Stable transfection of A431 cells with H2B fused to GFP (K/H2B-GFP). *A*, K/H2B-GFP cells appear as a single population showing high green fluorescence intensity (solid line). To ensure uniformity, high GFP-positive cells were sorted after stable transfection. The dotted line represents untransfected A431 cells. *B*, Images in real time were collected by confocal microscopy. K/H2B-GFP live cells express H2B-GFP exclusively in the nucleus (*left panel* and data not shown). H2B-GFP appears in apoptotic blebs and bodies (*right panel*) after UVB irradiation. *C*, Incorporation of H2B-GFP into the nucleosome core. Determination of purity of total histone prep by Coomassie blue staining (*top panels*). Western blot of the same prep with anti-GFP Ab shows a band of 49-kDa molecular mass, which corresponds to the H2B-GFP fusion protein (*bottom panels*). Nontransfected A431 cells are shown as control (*left panels*). H2B-GFP fusion protein is not cleaved during apoptosis (see also Fig. 1*D*). *D*, Autoantigen H2B-GFP fusion proteins are not cleaved during apoptosis. Lysates from wild-type and K/H2B-GFP cell line were analyzed by Western blot with mouse monoclonal anti-GFP. The fusion protein was detected as a band of ~50 kDa (corresponding to autoantigen (19 kDa) plus GFP (30 kDa)) and was not cleaved during apoptosis induced by UVB irradiation. Bands in the *upper* side of the blot are not specific. Poly(ADP-ribose) polymerase cleavage detected by Western blot demonstrates that UVB irradiation induced apoptosis-specific cleavage of caspase substrates. *E*, Membrane flipping. K/H2B-GFP cells were untreated or UVB irradiated, harvested after 5 h ofincubation, and stained with AxV-allophycocyanin and PI.

zoom. Analysis and movie reconstitution were performed with the above software.

Confocal imaging. Fixed Alexa (647)-CD11c$^+$ DCs cells were transferred onto glass-bottom culture dishes (MatTek). DCs were randomly counted on at least 10 different fields with a ×60 oil objective, and analyzed with Laser Sharp 2000 software (Bio-Rad).

Statistics

Differences in mean values between two groups were evaluated with two-tailed Student's *t* tests. The Microsoft Excel statistical package was used. Values of $p \leq 0.05$ were considered statistically significant.

Results

The H2B-GFP fusion protein is a reliable tool to study SLE autoantigens during apoptosis

To follow in real time, without sample fixation, the redistribution of SLE Ags during the apoptotic process, we generated stably transfected A431 keratinocytes expressing GFP fused with the H2B protein (K/H2B-GFP). H2B is a SLE-autoantigen (30) constituting part of the nucleosomal core (31). This approach allows real-time localization of H2B during apoptosis and its quantification in both nuclear and cytoplasmic compartments (L. Mcphie, D. Michel, J. Pehrson, and R. Caricchio, manuscript in preparation).

K/H2B-GFP cells were highly fluorescent (Fig. 1*A*). In live cells, the H2B-GFP fusion protein was expressed exclusively in the nucleus (Fig. 1*B*, *left panel*), as previously shown (32). This was confirmed by colocalization of fusion protein with native endogenous H2B, as demonstrated by intracellular staining of K/H2B-GFP cells with an anti-H2B Ab and by DRAQ5 (Biostatus Limited) staining, a red fluorescent cell-permeable DNA probe (data not shown). After induction of apoptosis by UVB, H2B-GFP was redistributed into apoptotic blebs and bodies (Fig. 1*B*, *right panel*).

To test whether the H2B-GFP fusion protein, as expected, was associated with the chromatin nucleosomal structure (32, 33), we isolated nuclei from transfected and from control cells and then extracted and purified chromatin. We then tested whether the resulting nucleosomes contained H2B-GFP fusion protein, and whether the latter was preserved during apoptosis. We extracted total histones from purified chromatin with sulfuric acid, as shown by Coomassie blue staining (Fig. 1*C*, *top*), and blotted histone preparations with an anti-GFP Ab (28). Anti-GFP Abs bound to a protein of 49 kDa which was present only in extracts from transfected cells (Fig. 1*C*, *bottom*). Forty-nine kilodaltons corresponds to the molecular mass of H2B (19 kDa) fused with GFP (30 kDa). We also checked the integrity of the fusion protein before and after induction of apoptosis by Western blot and found that our fusion protein was not cleaved during apoptosis (Fig. 1*D*).

Membrane flipping, blebbing, and chromatin condensation characterize early stages of apoptosis (34) and have been demonstrated previously in the parental A431 cells (34). To verify that K/H2B-GFP cells were capable of exposing membrane phospholipids, a potent eat-me signal for phagocytic cells (34), we exposed K/H2B-GFP cells to a dose of 15 mJ/cm^2 UVB, as previously described (24). Five hours after irradiation, we stained transfected cells with AxV and PI (Fig. 1*E*), a standard approach to distinguish early apoptosis (AxV positive, PI negative) from late apoptosis or from necrosis, where membrane integrity is lost (i.e., AxV and PI positive) (24). As shown in Fig. 1*E*, most irradiated K/H2B-GFP cells were in the early stages of apoptosis.

These data demonstrate that H2B-GFP localizes to the nucleus and is associated with the nucleosomal structure of live cells. During apoptosis, membrane flipping and nuclear fragmentation occur normally in K/H2B-GFP cells, and H2B-GFP, like its endogenous H2B counterpart (not shown), redistributes from the nucleus to apoptotic blebs. These observations support the usage of our fusion protein as a real-time tracer for both H2B and apoptotic nucleosomes.

H2B-GFP fusion protein is exposed on the cell surface during UVB-induced apoptosis and becomes accessible to lupus autoantibodies

It has been proposed that apoptotic blebs and bodies are potential sources of lupus autoantigens (21) and targets for autoantibodies (35). We therefore tested whether the H2B-GFP protein might become accessible to lupus autoantibodies during apoptosis. We used a monoclonal anti-H2B Ab (26) and stained cells without previous permeabilization (Fig. 2, thick line) to mimic in vivo conditions. We analyzed both UVB-irradiated and untreated K/H2B-GFP cells using gates to distinguish live and apoptotic cells (34). Only apoptotic cells showed anti-H2B Ab binding. Because the cells were in the early phases of apoptosis and maintained their membrane integrity (i.e., PI negative; see Fig. 1*E*), it is likely that the anti-histone Ab bound the cell surface-associated H2B and did not traverse the plasma membrane. Moreover, because live cells in the UVB-treated samples did not stain for H2B, it is unlikely that staining was the result of the release and adherence from morbid cells onto the surface of live cells (Fig. 2). These data have been also confirmed by confocal microscopy; apoptotic cells were incubated with anti-H2B or isotype control in complete medium, and then visualized with anti-mouse IgG, Alexa (647) conjugated (data not shown).

These data confirm and extend previous results showing that lupus autoantibodies can bind to the surface of apoptotic cells upon exposure of cytoplasmic and nuclear autoantigens during apoptosis (20, 21, 35).

Lupus autoantibodies enhance phagocytosis of apoptotic cells by DCs via FcγR uptake

We hypothesized that display of lupus autoantigen during apoptosis allows circulating autoantibodies to opsonize apoptotic cells and consequently enhances phagocytosis by DCs. This enhanced phagocytosis could increase nuclear autoantigen presentation by

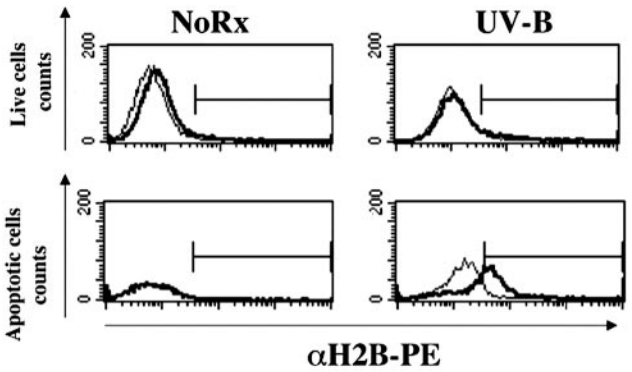

FIGURE 2. Nuclear SLE autoantigens translocate to the cellular membrane during apoptosis and are accessible to SLE autoantibodies. K/H2B-GFP cells were UVB irradiated, harvested after 6 h, and stained without previous permeabilization. A mouse monoclonal anti-H2B Ab (thick line) or an irrelevant isotype-matched control Ab (thin line) was used, followed by staining with a secondary PE-conjugated Ab. Cells were gated on forward scatter/side scatter for live cells (*upper panels*) or apoptotic cells (*lower panels*). After UVB irradiation, only apoptotic K/H2B-GFP cells (*lower right panel*) were positive for H2B, suggesting that the nuclear autoantigen not only localizes in the apoptotic blebs but also is displayed by the blebbing membrane. The data are representative of three different experiments.

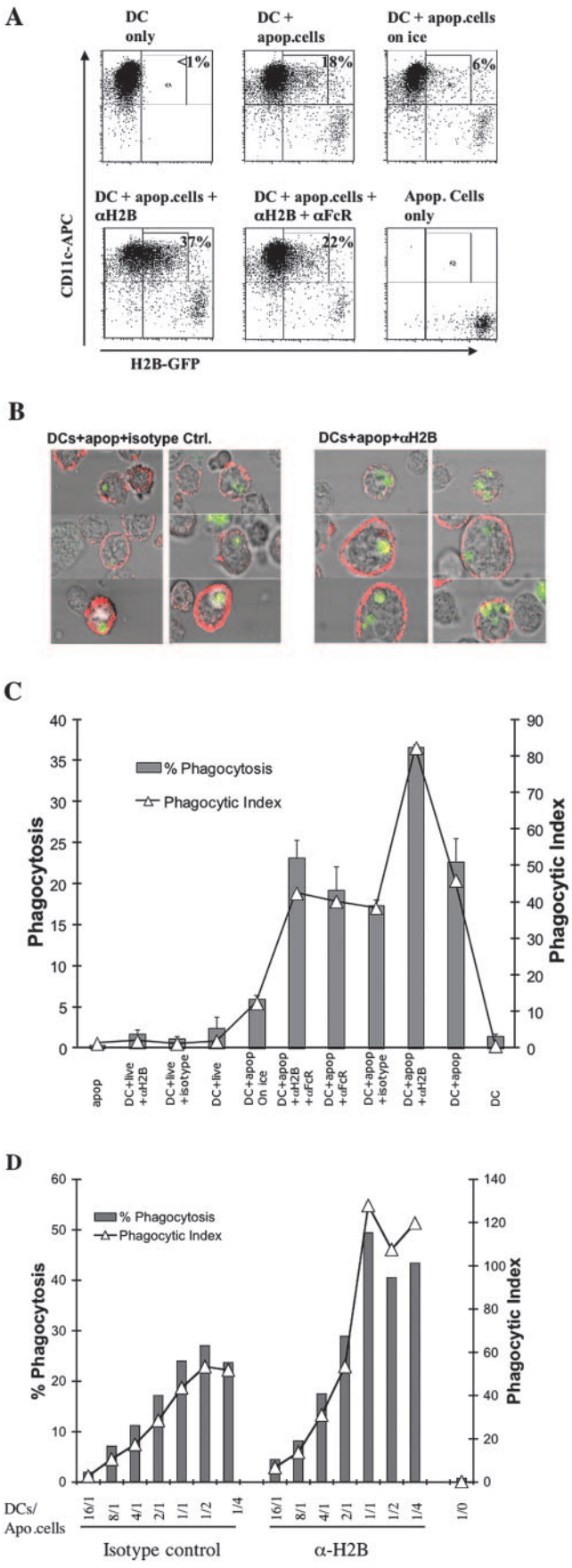

FIGURE 3. DC phagocytosis of apoptotic cells is enhanced by the display of nuclear autoantigen H2B via opsonization with SLE autoantibody and FcR-mediated uptake. K/H2B-GFP cells were UVB irradiated, incubated for 4 h, harvested, and seeded on bone marrow-derived DCs. After 2-h incubation at 37°C, cells were collected and stained for the DC marker CD11c. Resting DCs were >90% positive for CD11c. *A*, Representative plots of six different phagocytosis experiments, conducted with six independent bone marrow-derived DC (BMDC) cultures, are shown. DCs that had phagocytosed apoptotic K/H2B-GFP were double positive for CD11c and GFP. *B*, Confocal microscopy. BMDCs were incubated with apoptotic cells opsonized with anti-H2B or the isotype control. After the phagocytosis assay, cells were stained with anti-CD11c and visualized with streptavidin-Alexa (647). BMDC were then imaged and GFP-positive DC were counted to determine the phagocytic percentage and Ph.I. *C*, Percentage of phagocytosis (▨) and Ph.I. (line: Ph.I. = ((MFI-GFP × CD11c-GFP)/100)) (see *Materials and Methods* for details) are compared with demonstrate increase of phagocytic material after nuclear autoantibody opsonization. *D*, Percentage of phagocytosis (▨) and Ph.I. (line: Ph.I. = ((CD11c-GFP × ΔDC)/100)) (see *Materials and Methods* for details) of different DC/apoptotic cell ratios; phagocytosis saturation was achieved with a ratio of 1:2; at this and higher ratios, autoantibody opsonization still contributed to the enhancement of phagocytosis.

DCs. To test this, we first measured phagocytosis by immature/resting DCs of apoptotic cells opsonized with SLE anti-H2B autoantibodies.

We derived resting DCs from bone marrow precursors as previously described (17). At day 6 of culture, resting DCs are fully differentiated and highly phagocytic. They express high levels of FcγRIIb/III (not shown), express low levels of MHC class II and costimulatory molecules, and are promptly activated upon stimulatory signals such as LPS (36).

When we incubated resting DCs with UVB-induced apoptotic K/H2B-GFP cells (Fig. 3*A*) at a ratio of 2:1 for 2 h at 37°C, the DCs phagocytosed the apoptotic material. The phagocytosing cells were CD11c/GFP double-positive and accounted for 18% of gated cells. The uptake of apoptotic cells was FcγR independent, because DC pretreatment with an anti-FcγR Ab did not alter this process (Fig. 3*A*). Specific opsonization of the apoptotic cells with anti-H2B Ab induced a dramatic increase in the percentage of engulfing DCs, in comparison to the isotype control Ab (37 vs 17%; $p = 0.01$) (Fig. 3, *A* and *C*). These findings were further confirmed by confocal microscopy, which allowed direct visualization and counting of the bodies within the phagocytic cells (Fig. 3*B* and Table I). This approach also allowed estimating the amount of bodies attached rather than internalized; we found that, in all conditions tested, attached bodies constituted ≤5% of the total amount phagocytosed (Table I). The enhancement of phagocytosis was FcγR mediated, because the effect was reversed by pretreatment of DCs with an anti-FcγR blocking Ab (clone 2.4G2) ($p = 0.02$; Fig. 3, *A* and *C*). To exclude passive diffusion of H2B-GFP from cell to cell, we conducted experiments at 4°C instead of 37°C. The low temperature did not permit uptake of apoptotic material, consistent with an active process by DCs (Fig. 3, *A* and *C*). Notably, we did not observe phagocytosis by DCs of live keratinocytes opsonized or not (Fig. 3*C*).

We next analyzed the MFI within the GFP-positive CD11c cells to determine whether autoantibody opsonization increased phagocytosis within the same phagocytic cells or triggered phagocytosis in a larger number of DCs. The amount of material phagocytosed per cell was expressed as Ph.I. (see *Materials and Methods*), and, as shown in Fig. 3*C*, the Ph.I. completely overlapped with the percentage of phagocytosis, demonstrating that autoantibodies also increased the uptake of apoptotic material per individual phagocytic cell. Moreover, our results did not reflect immune complexes uptake due to release of chromatin or DNA in the medium. That is because, as previously published (24), in our system a 15 mJ/cm^2 UVB dose induced apoptosis and subsequent DNA fragmentation,

Table I. *Autoantibody opsonization and DC phagoytosis analysis by confocal microscopy*[a]

	Phagocytic Cells (%)[b]	Ph.I.[c]	Adherent Bodies (%)
DC + live + anti-H2B	6.2	0.06	3.1
DC + live + isotype	0	0	3
DC + live	0	0	0
DC + apop. on ice	3.1	0.03	3
DC + apop. + anti-H2B + anti-FcR	30.2	0.4	2.4
DC + apop. + anti-FcR	25	0.36	2.3
DC + apop. + isotype	24.3	0.26	2.7
DC + apop. + anti-H2B	46.3	0.98	4.8
DC + apop.	27.5	0.33	3.4
DC	0	0	0

[a] Abbreviation: apop., apoptotic.
[b] Note: % = ((number of $CD11c^+/GFP^+$ cells)/(100 $CD11c^+$ cells)).
[c] Note: Ph.I. = ((number of $CD11c^+/GFP^+$ cells) × (mean number of bodies per DC)/100)).

but chromatin was not released in the medium, as opposed to cells rendered necrotic with an 80 mJ/cm^2 UVB dose (24).

Finally, to ensure that the autoantibody-enhanced phagocytosis was independent from the ratio of DC/apoptotic cells, we performed a dose/response curve in which we progressively increased the amount of apoptotic cells. We found that autoantibody opsonization doubled the percentage of phagocytosis and the Ph.I. at any ratio used, even when the phagocytic capability of DCs was saturated (Fig. 3*D*). It is worthy to note that both routes of phagocytosis (via FcγR and via eat-me signals) were saturated at the same ratio of DCs/apoptotic cells (1:2), suggesting that they do not compete, but rather that they are completely independent processes. In summary, our results indicate that autoantibody opsonization increased the percentage of phagocytic DCs and induced higher apoptotic uptake within the same phagocytic population, therefore directly contributing to the increase of self-Ag loading.

Apoptotic bodies and blebs are a preferred phagocytic target of DCs

It is likely that, in vivo, tissue cells undergoing apoptosis, such as keratinocytes in the skin, are of the same size or considerably larger than resident DCs, potentially jeopardizing their phagocytic uptake and, thus, presentation of their Ags.

The morphologic sequence of apoptosis is well defined and is characterized by nuclear condensation and fragmentation, cytoplasmic contraction, and membrane surface blebbing where cellular components are packed and budded from the cell as small apoptotic bodies or blebs (14, 25, 37). The latter dramatic morphological changes might facilitate phagocytosis and digestion of this material by scavenger cells. This idea prompted us to investigate whether blebs and small bodies were indeed the preferred vehicle for Ag acquisition by DCs from dying cells. We measured DC uptake of apoptotic cells and large bodies vs apoptotic blebs and small bodies. We first separated apoptotic blebs and bodies from apoptotic cells by serial centrifugation (25). Fig. 4*A* shows by light microscopy and forward/side scatter that our separation yielded a preparation of enriched apoptotic bodies and blebs. We added equal amounts of apoptotic cells or apoptotic blebs/bodies, quantified according to total protein content, to DCs. We found that apoptotic bodies and blebs were phagocytosed almost twice as much as whole apoptotic cells ($p = 0.01$), and that opsonization with anti-H2B Ab further increased their uptake ($p = 0.04$) (Fig. 4*B*); these results were also confirmed by the higher Ph.I. (line). To ensure that the increase in GFP positivity of DCs that phagocytosed apoptotic

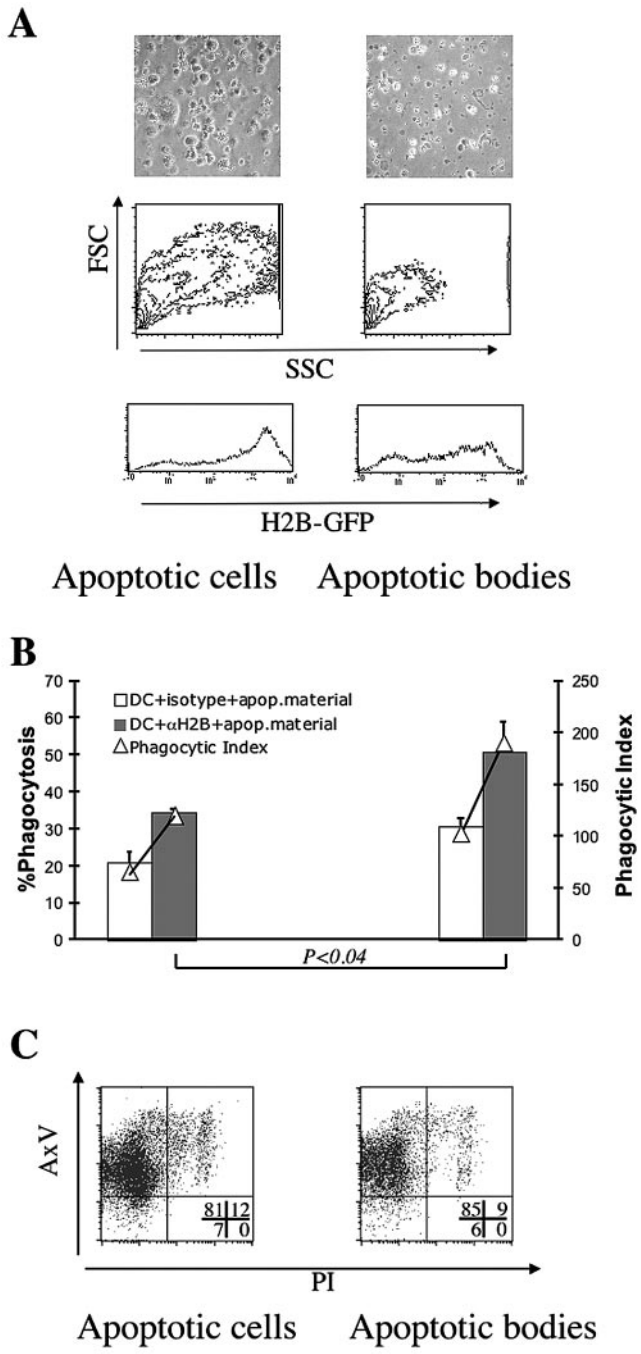

FIGURE 4. Apoptotic bodies and blebs are a preferred phagocytic target of DCs. K/H2B-GFP cells were UVB irradiated, and after 5-h incubation time, cells were separated into apoptotic blebs and apoptotic bodies by serial centrifugation. *A*, Forward- and side-scatter plots show that apoptotic bodies had a much lower scatter than apoptotic cells (*upper panels*). Phase contrast microscopy shows their smaller size (*lower panels*). *B*, K/H2B-GFP apoptotic cells and apoptotic blebs were proportionally diluted according to total protein content and seeded on DCs. Bar histograms show means and SDs of percentages of DC phagocytosis of anti-H2B or isotype control opsonized apoptotic cells or bodies. Apoptotic bodies, opsonized with lupus autoantibodies, were more phagocytosed than apoptotic cells. Bar histograms show means and SDs of duplicates from three distinct experiments, conducted with three independent bone marrow-derived DC cultures; the line is representative of the Ph.I. *C*, K/H2B-GFP apoptotic cells (*left panel*) and apoptotic blebs (*right panel*) were stained for AxV and PI as described in *Materials and Methods*.

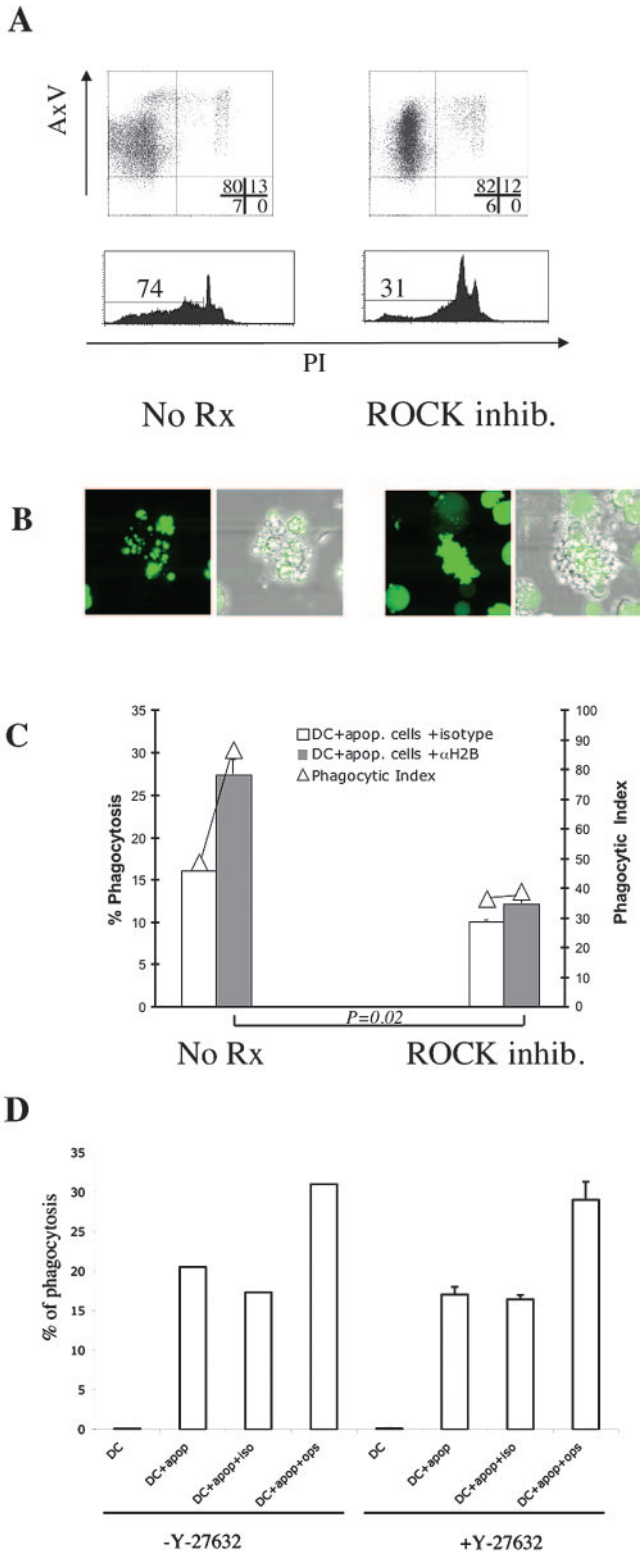

FIGURE 5. Nuclear autoantigen redistribution during apoptosis depends on chromatin fragmentation, and is necessary for autoantibody opsonization and enhanced DC phagocytosis of apoptotic cells. K/H2B-GFP cells were treated with the ROCK I and chromatin fragmentation inhibitor Y27623 for 1 h, UVB irradiated, and then rested for 5 h. *A*, AxV and PI staining plots (*upper panels*). AxV binding and PI permeability were no different under the two conditions, whereas chromatin fragmentation was greatly reduced, as indicated by reduction of the sub-G_0 peak (*lower panels*). *B*, Live confocal images of K/H2B-GFP cells show apoptotic K/H2B-GFP cells fragmented in multiple bodies and blebs, as indicated by the green color of H2B-GFP redistributed from the original nuclear location (*left panels* and Fig. 1*B*). Overlap of differential interphase contrast and fluorescence (*right panels*) also clearly shows that the nucleus fragments during apoptosis, and that its content redistributes within bodies and blebs, as shown by H2B-GFP fluorescence in blebs and bodies. In contrast, although apoptotic K/H2B-GFP cells pretreated with ROCK I inhibitor do form blebs, the nucleus does not fragment, and there is no redistribution of H2B-GFP within these blebs, as shown by the nucleus integrity and the lack of fluorescence in the blebs (*right panels*). *C*, Bar histograms and SDs of percentages of DC phagocytosis of anti-H2B or isotype control opsonized apoptotic cells, pretreated or not with ROCK I inhibitor. The data are averages of duplicates from three distinct experiments, conducted with three independent bone marrow-derived DC cultures; the line represents the Ph.I. calculated as in *Materials and Methods*. *D*, Y27632 treatment does not influence DC phagocytosis. DCs were coincubated for 2 h with apoptotic K/H2B-GFP cells, and then opsonized with anti-H2B or an isotype control. DCs were also pretreated with Y27632 (50 mM) to investigate its impact on the phagocytic capability of DCs. Cells were then stained for CD11c, and the percentage of phagocytosis and Ph.I. were measured.

blebs and bodies vs apoptotic cells was not due to different concentrations of H2B-GFP within the two apoptotic preparations, we determined its extent by flow cytometry. We found that apoptotic blebs and bodies had a lower MFI than the apoptotic cells (Fig. 4*A*, *lower panels*). These results suggest that the increase in phagocytosis of apoptotic blebs and bodies is not due to their higher MFI, but rather to a real increase in uptake (Fig. 4*A*, *lower panels*).

To determine the mechanism underlying this preferred phagocytosis, we compared expression by apoptotic blebs and bodies and whole apoptotic cells of a key eat-me signal, exposure of phospholipids (38) (Fig. 4*C*). The lack of difference in AxV binding and PI positivity excluded this as a factor in the uptake of apoptotic material and suggested that cell size might be important.

By real-time confocal microscopy, we confirmed that DCs phagocytosed mainly blebs and bodies. DCs moved about vigorously in the medium, extending their numerous dendrites and touching surrounding cells; DCs appeared to search for apoptotic blebs, and then find and detach the blebs from apoptotic cells and finally engulf them (data not shown). Taken together, our data suggest that apoptotic blebs and bodies are a preferred target of DC phagocytosis, via both eat-me signals and FcγR-mediated mechanisms.

Blockade of chromatin fragmentation eliminates the enhancement of phagocytosis induced by autoantibody opsonization

The biological mechanisms underlying nuclear autoantigen redistribution into blebs and bodies of dying cells are unknown (39), although one hypothesis is that autoantigen redistribution is an event downstream from chromatin fragmentation (40). We hypothesized that chromatin fragmentation is mandatory for histone relocation to apoptotic blebs, and is required for the FcγR-mediated enhancement of phagocytosis of autoantibodies-opsonized apoptotic cells. Therefore, blockade of chromatin fragmentation in lupus could limit DC access to autoantigens from apoptotic cells.

To test our hypothesis, we inhibited chromatin fragmentation by blocking ROCK I (41). ROCK I inhibition was chosen because it does not interfere with the exposure of membrane phospholipids (40) necessary to trigger phagocytosis via scavenger receptors (42). As shown in Fig. 5*A*, *upper panels*, apoptotic K/H2B-GFP cells exposed similar amounts of phospholipids with or without treatment with the ROCK I inhibitor Y27632, making possible similar basal levels of phagocytosis by DCs. In contrast, chromatin fragmentation was dramatically reduced by Y27632, as shown by the marked decrease in sub-G_0 DNA (Fig. 5*A*, *lower panels*). No

appreciable effect was noticed when nonirradiated K/H2B-GFP cells were incubated with Y27623 (data not shown). The reduction in chromatin fragmentation resulted in the inhibition of translocation of H2B-GFP fusion protein to the apoptotic blebs (Fig. 5*B*). When we determined the effects of ROCK I inhibitor on phagocytosis of apoptotic cells by DCs, we found that the blockade of chromatin fragmentation eliminated the enhancement of phagocytosis induced by autoantibody opsonization ($p = 0.02$), whereas it did not affect the baseline level of phagocytosis of unopsonized apoptotic cells (p = NS) (Fig. 5*C*). We have obtained similar results by using Zn^{2+}, a nonspecific endonuclease inhibitor that blocks chromatin and nuclear fragmentation during cell death (data not shown and Ref. 34). Although the latter results suggest that Y27632 affected only the process of apoptotic chromatin fragmentation and not the capacity of DCs to phagocytose, we further tested this possibility by pretreating DCs with the ROCK I inhibitor and then measuring their phagocytosis of fragmented apoptotic K/H2B-GFP cells. We found that pretreatment of DCs with Y27632 did not decrease phagocytosis of apoptotic cells by DCs (Fig. 5*D*).

These data further support our hypothesis that lupus autoantibodies enhance DC phagocytosis of apoptotic cells because redistribution of nuclear autoantigens during apoptosis promotes autoantigen accessibility. Furthermore, the processes of chromatin fragmentation and autoantigen redistribution are linked: by inhibiting a kinase required for chromatin fragmentation, we blocked autoantigen redistribution, and also its enhancement of FcγR-mediated phagocytosis.

Apoptotic cells opsonized with lupus autoantibodies enhance DC Ag presentation

We hypothesized that the enhanced phagocytosis, induced by opsonization of apoptotic cells by lupus autoantibodies could also enhance autoantigen presentation. This mechanism could turn into a powerful vicious circle capable of sustaining and amplifying autoreactive T cell stimulation and autoantibody production from autoreactive B cells, thus maintaining the autoimmune disease.

To investigate this possibility, we tested the in vitro capability of DCs fed with apoptotic K/H2B-GFP cells to restimulate CD4-positive T cells specific for nuclear Ags expressed by apoptotic cells. To overcome the absence of T cell clones specific for H2B derived from C57BL/6 mice and avoid mechanisms of suppression/regulation in place in non-autoimmune mice, we decided to test the specific response to GFP fused to H2B. We immunized mice with GFP, and 3 wk postimmunization, all three mice developed anti-GFP Abs, demonstrating an effective immune response against GFP (data not shown). We coincubated T cells isolated from GFP-immunized mice with DCs that had previously phagocytosed apoptotic cells opsonized with anti-H2B or isotype control Abs and then induced to activate by mechanical stress, using a protocol (transfer) that we and other have shown to induce full DC maturation (data not shown and Refs. 17 and 43).

To track T cell divisions, we used CFSE, a dye that segregates equally between daughter cells upon cell division, resulting in the sequential halving of cellular fluorescence intensity with each successive generation (29). We observed that a significantly higher proportion of CD4 T cells underwent specific proliferation when stimulated by DCs fed with apoptotic cells opsonized with anti-H2B Abs than with the isotype control or with unfed DCs ($p = 0.01$ and $p = 0.008$, respectively; Fig. 6). To our knowledge, this is the first demonstration that SLE autoantigen redistribution has the immunological consequence of increasing nuclear Ag presentation to T cells.

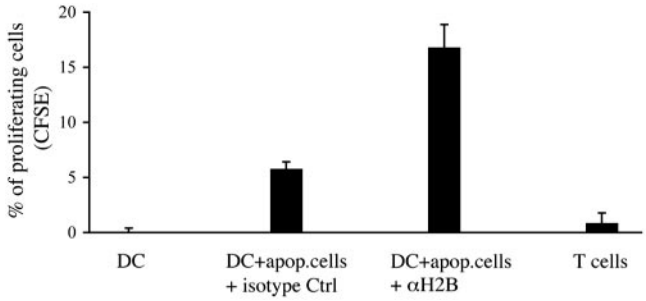

FIGURE 6. Increased DC phagocytosis of opsonized apoptotic cells leads to enhanced autoantigen presentation and T cell proliferation. CD4 T lymphocytes proliferation was used as read-out system to assess the Ag presentation capability of DCs after phagocytosis. Bar histograms show the relative averages of the percentages of CD4 proliferating cells. CD4 T cells exposed to DCs that had phagocytosed opsonized apoptotic cells showed the highest percentage of cells ($p = 0.01$ and $p = 0.008$, respectively). Data are from a representative experiment in duplicate.

Discussion

We report here that autoantibodies specific for nuclear autoantigens increase Ag presentation by delivering apoptotic blebs and bodies to DCs via FcγR-mediated phagocytosis. To our knowledge, this is the first demonstration that autoantibody binding to lupus nuclear autoantigens on the surface of apoptotic cells induces a specific form of phagocytosis and consequent Ag presentation.

FcγR-mediated phagocytosis has been shown to be proinflammatory (44, 45) and extremely efficient in Ag clearance and loading for presentation by DCs (46). Our data suggest that autoantibodies specific for nuclear autoantigens can deliver apoptotic material and, possibly, a proinflammatory signal to DCs by promoting FcγR-mediated phagocytosis. Although the focus of this paper is the physiologic apoptosis as source of Ag in lupus, we have obtained similar results with DCs fed with cells rendered necrotic by UVB (data not shown and Ref. 24), suggesting that necrosis as well can deliver nuclear material, probably via uptake of immune complexes (24); we are actively investigating the role of necrosis in SLE. Furthermore, our results support the important role of FcγRs in SLE, already established in the NZB/W mouse model (47). Moreover, interestingly, the increased uptake of apoptotic material upon opsonization had a major effect on DC capacity to stimulate T cells specific for GFP, suggesting that this phenomenon may have important functional consequences for the maintenance of the autoimmune process. Indeed, DCs fed with apoptotic cells opsonized with anti-H2B autoantibodies induced a stronger T cell response then those fed with apoptotic cells incubated with isotype control Abs. Boulé et al. (44) have recently shown that nucleosomes-IgG immune complexes can activate DCs. To single out the role of phagocytosis and Ag loading on Ag presentation, and allow presentation of nonopsonized apoptotic cells, which we have previously shown cannot be presented by resting DCs (17), we induced activation in DCs by mechanical stress (transfer) (data not shown and Ref. 17). Although we cannot exclude a role for differences in DC costimulatory power, induced by opsonized vs nonopsonized apoptotic cells, the results of the different amounts of phagocytosis lead us to propose that the observed differences in T cell response were at least partially, if not mostly, due to Ag loading and display by DCs. This hyperloading of self-Ags, coupled with DC activation via TLR9-FcγR as suggested by Boulé et al. (44), could have important pathologic consequences in SLE.

Our results also increase our understanding of the nature of the apoptotic material ingested by DCs. Blebs and small apoptotic bodies budding from dying cells, rather than intact or nearly intact cells, appear to be the major DC phagocytic targets. DC uptake is constant and is required for tolerance maintenance and cross-presentation (48, 49). By live confocal imaging, we observed that DCs mainly detach blebs and small bodies from apoptotic cells, apparently because they have a more "eatable" size. This must be a widespread ongoing process of fundamental importance, analogous to the "sampling" behavior of DCs observed in Ag-stimulated lymph nodes (50–52). In view of the massive amount of apoptotic debris generated constitutively, laden as it is with nuclear autoantigens, it must be critical that material acquired in such a manner not trigger an immunogenic phenotype in DCs. The presence of even small amounts of antinuclear Abs might serve to opsonize such debris and favor a vigorous immune response, thereby exacerbating autoimmunity.

Our results also bear on more general aspects of autoantigen redistribution and its significance. It has occurred to us that Ag redistribution may have the effect of turning dying cells "inside out." In the case of dying cells infected by viruses or other intracellular parasites, Ag redistribution could expose otherwise-hidden intracellular viral or microbial Ags to anti-pathogen Abs, thereby promoting APC phagocytosis, viral Ag presentation, and clearance. Therefore, apoptotic intracellular exposure may contribute in a favorable way to host defense, particularly secondary immune responses against foreign Ags at a time when Ab already exists.

In lupus-prone individuals, in whom autoantibodies may be present years before the onset of disease (53), nuclear autoantigen redistribution into blebs and bodies could serve as an opsonization target for autoantibodies, which in turn amplify the uptake and presentation of self-Ag. Over the years, multiple precipitating events, such as repeated exposures to UVB light (24), could cause the genetically predisposed individual to overcome tolerance and develop full-blown lupus. Thus, a mechanism such as nuclear Ag translocation, that might have evolved to boost phagocytosis of virally infected cells, may also be a major pathogenic component of lupus autoimmunity.

Under this scenario, nuclear autoantigen redistribution into blebs and bodies and/or these subcellular structures themselves could be lupus therapeutic targets. To test this possibility, we used Y27632, a specific inhibitor of ROCK I. ROCK I is the effector kinase of Rho and is a multifunctional protein involved in many aspects of cell motility: stress-fiber formation and contraction, cell adhesion, migration and invasion, cell size and differentiation (41). However, its pertinent involvement during apoptosis is in chromatin and nuclear fragmentation, blebbing formation, and redistribution of fragmented chromatin into blebs and bodies (40, 54). Y27632 treatment inhibits ROCK I, and thereby abolishes chromatin and nuclear fragmentation, but does not interfere with phospholipid exposure, as shown by our results (Fig. 5) and previous work (40). Inhibition of ROCK I via Y27632 has been also shown to inhibit membrane blebbing, although in our experiments, it did not appear to be the case (Fig. 5*B*). The latter results are probably due to differences in susceptibility among cell lines; nevertheless, in our experiments chromatin and nuclear fragmentation was indeed inhibited by Y27632 and so was redistribution of nuclear material into blebs and bodies (Fig. 5).

The consequence of this inhibition is a specific decrease of the uptake of opsonized bodies and blebs by DCs, while leaving intact the phagocytosis of nonopsonized cells. Inhibition of autoantigen redistribution is a potential therapeutic strategy to decrease availability to the immune system of autoantigens taken up in a proinflammatory fashion while leaving available for tolerization those autoantigens delivered in a noninflammatory context. Another advantage of blocking nuclear autoantigen redistribution is that, among the multiple steps of the apoptotic cascade, only chromatin fragmentation and possibly blebs formation are inhibited, whereas the remaining processes are not affected, as far as we know, and can proceed to the fundamental function of disposing of unwanted cells The treatment might thus lead to a reduction or termination of the autoimmune response in lupus, by subtracting autoantigens from the immunogenic route that fuels autoimmunity and helping to re-establish tolerance.

Acknowledgments

We thank Drs. Philip Cohen, Robert Eisenberg, Terri Finkel, and Terri Laufer for their support and for critically reading the manuscript, and Drs. Madesh Muniswamy and Qin Shi for being instrumental in the live imaging experiments.

Disclosures

The authors have no financial conflict of interest.

References

1. Tan, E. M., and H. G. Kunkel. 1966. Characteristics of a soluble nuclear antigen precipitating with sera of patients with systemic lupus erythematosus. *J. Immunol.* 96: 464–471.
2. Plotz, P. H. 2003. The autoantibody repertoire: searching for order. *Nat. Rev. Immunol.* 3: 73–78.
3. Mevorach, D., J. L. Zhou, X. Song, and K. B. Elkon. 1998. Systemic exposure to irradiated apoptotic cells induces autoantibody production. *J. Exp. Med.* 188: 387–392.
4. Cohen, P. L., R. Caricchio, V. Abraham, T. D. Camenisch, J. C. Jennette, R. A. Roubey, H. S. Earp, G. Matsushima, and E. A. Reap. 2002. Delayed apoptotic cell clearance and lupus-like autoimmunity in mice lacking the c-mer membrane tyrosine kinase. *J. Exp. Med.* 196: 135–140.
5. Korb, L. C., and J. M. Ahearn. 1997. C1q binds directly and specifically to surface blebs of apoptotic human keratinocytes: complement deficiency and systemic lupus erythematosus revisited. *J. Immunol.* 158: 4525–4528.
6. Prodeus, A. P., S. Goerg, L. M. Shen, O. O. Pozdnyakova, L. Chu, E. M. Alicot, C. C. Goodnow, and M. C. Carroll. 1998. A critical role for complement in maintenance of self-tolerance. *Immunity* 9: 721–731.
7. Bickerstaff, M. C., M. Botto, W. L. Hutchinson, J. Herbert, G. A. Tennent, A. Bybee, D. A. Mitchell, H. T. Cook, P. J. Butler, M. J. Walport, and M. B. Pepys. 1999. Serum amyloid P component controls chromatin degradation and prevents antinuclear autoimmunity. *Nat. Med.* 5: 694–697.
8. Napirei, M., H. Karsunky, B. Zevnik, H. Stephan, H. G. Mannherz, and T. Moroy. 2000. Features of systemic lupus erythematosus in Dnase1-deficient mice. *Nat. Genet.* 25: 177–181.
9. Szondy, Z., Z. Sarang, P. Molnar, T. Nemeth, M. Piacentini, P. G. Mastroberardino, L. Falasca, D. Aeschlimann, J. Kovacs, I. Kiss, et al. 2003. Transglutaminase $2^{-/-}$ mice reveal a phagocytosis-associated crosstalk between macrophages and apoptotic cells. *Proc. Natl. Acad. Sci. USA* 100: 7812–7817.
10. Wilkinson, R., A. B. Lyons, D. Roberts, M. X. Wong, P. A. Bartley, and D. E. Jackson. 2002. Platelet endothelial cell adhesion molecule-1 (PECAM-1/CD31) acts as a regulator of B-cell development, B-cell antigen receptor (BCR)-mediated activation, and autoimmune disease. *Blood* 100: 184–193.
11. Hanayama, R., M. Tanaka, K. Miyasaka, K. Aozasa, M. Koike, Y. Uchiyama, and S. Nagata. 2004. Autoimmune disease and impaired uptake of apoptotic cells in MFG-E8-deficient mice. *Science* 304: 1147–1150.
12. Cohen, P. L., and R. Caricchio. 2004. Genetic models for the clearance of apoptotic cells. *Rheum. Dis. Clin. North Am.* 30: 473–486.
13. Arends, M. J., R. G. Morris, and A. H. Wyllie. 1990. Apoptosis. The role of the endonuclease. *Am. J. Pathol.* 136: 593–608.
14. Mills, J. C., N. L. Stone, and R. N. Pittman. 1999. Extranuclear apoptosis. The role of the cytoplasm in the execution phase. *J. Cell Biol.* 146: 703–708.
15. Mills, J. C., V. M. Lee, and R. N. Pittman. 1998. Activation of a PP2A-like phosphatase and dephosphorylation of tau protein characterize onset of the execution phase of apoptosis. *J. Cell Sci.* 111: 625–636.
16. Albert, M. L., B. Sauter, and N. Bhardwaj. 1998. Dendritic cells acquire antigen from apoptotic cells and induce class I- restricted CTLs. *Nature* 392: 86–89.
17. Gallucci, S., M. Lolkema, and P. Matzinger. 1999. Natural adjuvants: endogenous activators of dendritic cells. *Nat. Med.* 5: 1249–1255.
18. Casciola-Rosen, L. A., G. Anhalt, and A. Rosen. 1994. Autoantigens targeted in systemic lupus erythematosus are clustered in two populations of surface structures on apoptotic keratinocytes. *J. Exp. Med.* 179: 1317–1330.
19. LeFeber, W. P., D. A. Norris, S. R. Ryan, J. C. Huff, L. A. Lee, M. Kubo, S. T. Boyce, B. L. Kotzin, and W. L. Weston. 1984. Ultraviolet light induces binding of antibodies to selected nuclear antigens on cultured human keratinocytes. *J. Clin. Invest.* 74: 1545–1551.
20. Miranda, M. E., C. E. Tseng, W. Rashbaum, R. L. Ochs, C. A. Casiano, F. Di Donato, E. K. Chan, and J. P. Buyon. 1998. Accessibility of SSA/Ro and

SSB/La antigens to maternal autoantibodies in apoptotic human fetal cardiac myocytes. *J. Immunol.* 161: 5061–5069.
21. Radic, M., T. Marion, and M. Monestier. 2004. Nucleosomes are exposed at the cell surface in apoptosis. *J. Immunol.* 172: 6692–6700.
22. Fadok, V. A., and P. M. Henson. 2003. Apoptosis: giving phosphatidylserine recognition an assist–with a twist. *Curr. Biol.* 13: R655–R657.
23. Henson, P. M., D. L. Bratton, and V. A. Fadok. 2001. Apoptotic cell removal. *Curr. Biol.* 11: R795–R805.
24. Caricchio, R., L. McPhie, and P. L. Cohen. 2003. Ultraviolet B radiation-induced cell death: critical role of ultraviolet dose in inflammation and lupus autoantigen redistribution. *J. Immunol.* 171: 5778–5786.
25. Casciola-Rosen, L. A., D. K. Miller, G. J. Anhalt, and A. Rosen. 1994. Specific cleavage of the 70-kDa protein component of the U1 small nuclear ribonucleoprotein is a characteristic biochemical feature of apoptotic cell death. *J. Biol. Chem.* 269: 30757–30760.
26. Monestier, M., P. Decker, J. P. Briand, J. L. Gabriel, and S. Muller. 2000. Molecular and structural properties of three autoimmune IgG monoclonal antibodies to histone H2B. *J. Biol. Chem.* 275: 13558–13563.
27. Anderson, H. A., C. A. Maylock, J. A. Williams, C. P. Paweletz, H. Shu, and E. Shacter. 2003. Serum-derived protein S binds to phosphatidylserine and stimulates the phagocytosis of apoptotic cells. *Nat. Immunol.* 4: 87–91.
28. Changolkar, L. N., and J. R. Pehrson. 2002. Reconstitution of nucleosomes with histone macroH2A1.2. *Biochemistry* 41: 179–184.
29. Wells, A. D., H. Gudmundsdottir, and L. A. Turka. 1997. Following the fate of individual T cells throughout activation and clonal expansion: signals from T cell receptor and CD28 differentially regulate the induction and duration of a proliferative response. *J. Clin. Invest.* 100: 3173–3183.
30. Hardin, J. A., and J. E. Craft. 1987. Patterns of autoimmunity to nucleoproteins in patients with systemic lupus erythematosus. *Rheum. Dis. Clin. North Am.* 13: 37–46.
31. Mohan, C., S. Adams, V. Stanik, and S. K. Datta. 1993. Nucleosome: a major immunogen for pathogenic autoantibody-inducing T cells of lupus. *J. Exp. Med.* 177: 1367–1381.
32. Kanda, T., K. F. Sullivan, and G. M. Wahl. 1998. Histone-GFP fusion protein enables sensitive analysis of chromosome dynamics in living mammalian cells. *Curr. Biol.* 8: 377–385.
33. Kanno, T., Y. Kanno, R. M. Siegel, M. K. Jang, M. J. Lenardo, and K. Ozato. 2004. Selective recognition of acetylated histones by bromodomain proteins visualized in living cells. *Mol. Cell* 13: 33–43.
34. Caricchio, R., E. A. Reap, and P. L. Cohen. 1998. Fas/Fas ligand interactions are involved in ultraviolet-B-induced human lymphocyte apoptosis. *J. Immunol.* 161: 241–251.
35. Cocca, B. A., A. M. Cline, and M. Z. Radic. 2002. Blebs and apoptotic bodies are B cell autoantigens. *J. Immunol.* 169: 159–166.
36. Sallusto, F., M. Cella, C. Danieli, and A. Lanzavecchia. 1995. Dendritic cells use macropinocytosis and the mannose receptor to concentrate macromolecules in the major histocompatibility complex class II compartment: downregulation by cytokines and bacterial products. *J. Exp. Med.* 182: 389–400.
37. Savill, J., I. Dransfield, C. Gregory, and C. Haslett. 2002. A blast from the past: clearance of apoptotic cells regulates immune responses. *Nat. Rev. Immunol.* 2: 965–975.
38. Martin, S. J., C. P. Reutelingsperger, A. J. McGahon, J. A. Rader, R. C. van Schie, D. M. LaFace, and D. R. Green. 1995. Early redistribution of plasma membrane phosphatidylserine is a general feature of apoptosis regardless of the initiating stimulus: inhibition by overexpression of Bcl-2 and Abl. *J. Exp. Med.* 182: 1545–1556.
39. Pollard, K. M. 2002. Cell death, autoantigen cleavage, and autoimmunity. *Arthritis Rheum.* 46: 1699–1702.
40. Coleman, M. L., E. A. Sahai, M. Yeo, M. Bosch, A. Dewar, and M. F. Olson. 2001. Membrane blebbing during apoptosis results from caspase-mediated activation of ROCK I. *Nat. Cell Biol.* 3: 339–345.
41. Riento, K., and A. J. Ridley. 2003. Rocks: multifunctional kinases in cell behaviour. *Nat. Rev. Mol. Cell Biol.* 4: 446–456.
42. Fadok, V. A., D. R. Voelker, P. A. Campbell, J. J. Cohen, D. L. Bratton, and P. M. Henson. 1992. Exposure of phosphatidylserine on the surface of apoptotic lymphocytes triggers specific recognition and removal by macrophages. *J. Immunol.* 148: 2207–2216.
43. Inaba, K., M. Inaba, N. Romani, H. Aya, M. Deguchi, S. Ikehara, S. Muramatsu, and R. M. Steinman. 1992. Generation of large numbers of dendritic cells from mouse bone marrow cultures supplemented with granulocyte/macrophage colony-stimulating factor. *J. Exp. Med.* 176: 1693–1702.
44. Boulé, M. W., C. Broughton, F. Mackay, S. Akira, A. Marshak-Rothstein, and I. R. Rifkin. 2004. Toll-like receptor 9-dependent and -independent dendritic cell activation by chromatin-immunoglobulin G complexes. *J. Exp. Med.* 199: 1631–1640.
45. Amigorena, S. 2002. Fcγ receptors and cross-presentation in dendritic cells. *J. Exp. Med.* 195: F1–F3.
46. Dhodapkar, K. M., J. Krasovsky, B. Williamson, and M. V. Dhodapkar. 2002. Antitumor monoclonal antibodies enhance cross-presentation of Cellular antigens and the generation of myeloma-specific killer T cells by dendritic cells. *J. Exp. Med.* 195: 125–133.
47. Clynes, R., C. Dumitru, and J. V. Ravetch. 1998. Uncoupling of immune complex formation and kidney damage in autoimmune glomerulonephritis. *Science* 279: 1052–1054.
48. Kurts, C., H. Kosaka, F. R. Carbone, J. F. Miller, and W. R. Heath. 1997. Class I-restricted cross-presentation of exogenous self-antigens leads to deletion of autoreactive $CD8^+$ T cells. *J. Exp. Med.* 186: 239–245.
49. Banchereau, J., F. Briere, C. Caux, J. Davoust, S. Lebecque, Y. J. Liu, B. Pulendran, and K. Palucka. 2000. Immunobiology of dendritic cells. *Annu. Rev. Immunol.* 18: 767–811.
50. Itano, A. A., and M. K. Jenkins. 2003. Antigen presentation to naive CD4 T cells in the lymph node. *Nat. Immunol.* 4: 733–739.
51. Huang, A. Y., H. Qi, and R. N. Germain. 2004. Illuminating the landscape of in vivo immunity: insights from dynamic in situ imaging of secondary lymphoid tissues. *Immunity* 21: 331–339.
52. Mempel, T. R., S. E. Henrickson, and U. H. Von Andrian. 2004. T-cell priming by dendritic cells in lymph nodes occurs in three distinct phases. *Nature* 427: 154–159.
53. Arbuckle, M. R., M. T. McClain, M. V. Rubertone, R. H. Scofield, G. J. Dennis, J. A. James, and J. B. Harley. 2003. Development of autoantibodies before the clinical onset of systemic lupus erythematosus. *N. Engl. J. Med.* 349: 1526–1533.
54. Sebbagh, M., C. Renvoize, J. Hamelin, N. Riche, J. Bertoglio, and J. Breard. 2001. Caspase-3-mediated cleavage of ROCK I induces MLC phosphorylation and apoptotic membrane blebbing. *Nat. Cell Biol.* 3: 346–352.